

SUPPLEMENTARY MATERIALS FOR: UNIFORM MULTI-PENALTY REGULARIZATION FOR LINEAR ILL-POSED INVERSE PROBLEMS*

VILLIAM BORTOLOTTI[†], GERMANA LANDI[‡], AND FABIANA ZAMA [§]

Introduction. This document presents the supplementary materials for the article titled "Uniform Multi-Penalty Regularization for Linear Ill-Posed Inverse Problems" by Villiam Bortolotti, Germana Landi, and Fabiana Zama. The supplementary materials provide extended discussions on one-dimensional test problems. After the description of the test problems and algorithmic settings in section 1, low noise and high noise results are extensively discussed in sections 2 and 3 respectively.

1. One-dimensional test problems. Starting from a ground-truth signal $\mathbf{u}^* \in \mathbb{R}^N$, we generate the test problem by convolving it with a blurring operator $A \in \mathbb{R}^{M \times N}$ and then corrupting the blurred signal with additive Gaussian noise of level δ , i.e.

$$\mathbf{b} = \mathbf{y} + \text{noise}$$

where $\text{noise} = \delta \boldsymbol{\eta} \|\mathbf{y}\|$, with $\mathbf{y} = A\mathbf{u}^*$ and $\boldsymbol{\eta} \in \mathbb{R}^M$ a random normal vector with norm one. We consider two scenarios: a low-noise scenario corresponding to $\delta = 0.01$, and a high-noise scenario where $\delta = 0.1$. We define three test problems where each signal has different and progressively more complex features representing a challenge for the regularization functions.

- T1 The signal $\mathbf{u}^* \in \mathbb{R}^{100}$ and the linear operator $A \in \mathbb{R}^{100 \times 100}$ are obtained by the `heat` function from Hansen's Regularization Tools [1]. The ground truth \mathbf{u}^* , represented in Figure S1 (left), is a sparse signal with mostly zero values except for a single peak quite close to the axes origin.
- T2 The signal $\mathbf{u}^* \in \mathbb{R}^{404}$ (Figure S1, center) has two narrow peaks over a flat area and a smooth rounded area. The operator A represents a Gaussian blur with a standard deviation of five.
- T3 The signal $\mathbf{u}^* \in \mathbb{R}^{504}$ (Figure S1, right) presents a smooth rounded feature, a narrow peak and a ramp. The same Gaussian blur of T2 is used.

For these three test problems, we observe the behaviour of Algorithm UPenMM with $p = N$ penalty functions as follows:

$$(1.1) \quad \psi_i(\mathbf{u}) = (L\mathbf{u})_i^2 + \epsilon, \quad i = 1, \dots, N$$

where $L \in \mathbb{R}^{N \times N}$ is the discretization of the second order derivative operator and ϵ is a small positive constant in the range $[10^{-7}, 10^{-5}]$. Moreover, we analyse the generalized approach proposed in Algorithm GUPenMM with $\varepsilon = 0.9$, ψ_i as in (1.1)

*Submitted to the editors DATE.

Funding: This work was partially supported by the Istituto Nazionale di Alta Matematica, Gruppo Nazionale per il Calcolo Scientifico (INdAM-GNCS).

[†]Department of Civil, Chemical, Environmental, and Materials Engineering, University of Bologna, Via Terracini, 28, 40131 Bologna, Italy (villiam.bortolotti@unibo.it)

[‡]Department of Mathematics, University of Bologna, Piazza di Porta S. Donato 5, 40126 Bologna, Italy (germana.landi@unibo.it).

[§]Department of Mathematics, University of Bologna, Piazza di Porta S. Donato 5, 40126 Bologna, Italy (fabiana.zama@unibo.it).

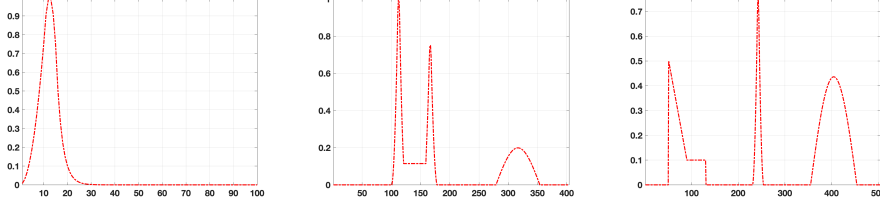


FIG. S1. 1D test problems: ground truth \mathbf{u}^* . Left T1, center T2, right T3.

and the following generalized regularization parameter $\tilde{\lambda}$:

$$(1.2) \quad \tilde{\lambda}_i = \frac{\|A\mathbf{u}_{\lambda} - \mathbf{b}\|^2}{N\tilde{\psi}_i(\mathbf{u}_{\lambda})}, \quad \tilde{\psi}_i(\mathbf{u}_{\lambda}) = \max \{\psi_{i-1}(\mathbf{u}_{\lambda}), \psi_i(\mathbf{u}_{\lambda}), \psi_{i+1}(\mathbf{u}_{\lambda})\}, \quad i = 1, \dots, N.$$

Both algorithms are tested in the unconstrained ($\Omega = \mathbb{R}^N$) and non-negatively constrained ($\Omega = \mathbb{R}_+^N$ where \mathbb{R}_+^N is the positive orthant) cases. A solution of the subproblem at step 3 of Algorithms UPenMM and GUPenMM has been computed, in the unconstrained case, by solving its first order conditions, while the Newton Projection method [2] has been used in the constrained case.

The initial values $\lambda_i^{(0)}$, $i = 1, \dots, N$, have been chosen such that

$$\lambda_i^{(0)} = \frac{\|A\mathbf{b} - \mathbf{b}\|^2}{N\psi_i(\mathbf{b})} \quad \text{for Algorithm UPenMM;}$$

$$\lambda_i^{(0)} = \frac{\|A\mathbf{b} - \mathbf{b}\|^2}{N\tilde{\psi}_i(\mathbf{b})} \quad \text{for Algorithm GUPenMM.}$$

2. Low-noise results. We begin by analyzing the behaviour of the two algorithms in the case of low noise, both in the unconstrained ($\Omega = \mathbb{R}^N$) and in the non-negatively constrained ($\Omega = \mathbb{R}_+^N$) scenarios. To show the amount of noise on the blurred data we represent in Figure S2 the blurred noisy data \mathbf{b} (blue line), and the blurred data \mathbf{y} .

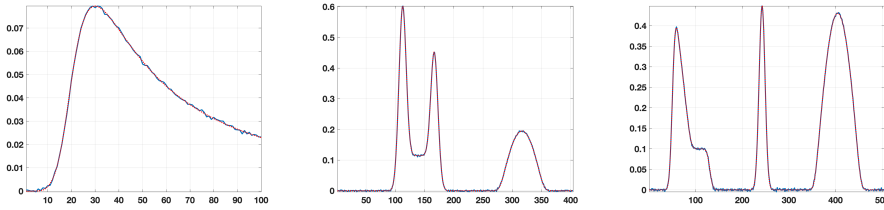


FIG. S2. 1D test problems ($\delta = 0.01$). Blue line: blurred noisy data \mathbf{b} , dotted red line: blurred data \mathbf{y} . Left T1, center T2, right T3.

A first evaluation of the methods is made by inspecting the error history represented in Figure S3(a) when $\Omega = \mathbb{R}^N$ and in Figure S3(b) for $\Omega = \mathbb{R}_+^N$. Each picture shows the relative error curves of Algorithm UPenMM (black dash-dot line) and Algorithm GUPenMM (blue dashed line). The red dots represent the relative error values corresponding to the following **stopping criterion**:

$$(2.1) \quad \|\lambda^{(k+1)} - \lambda^{(k)}\| \leq \|\lambda^{(k)}\| Tol_{\lambda}$$

with $Tol_\lambda = 10^{-2}$. We can appreciate the positive influence of the modified evalua-

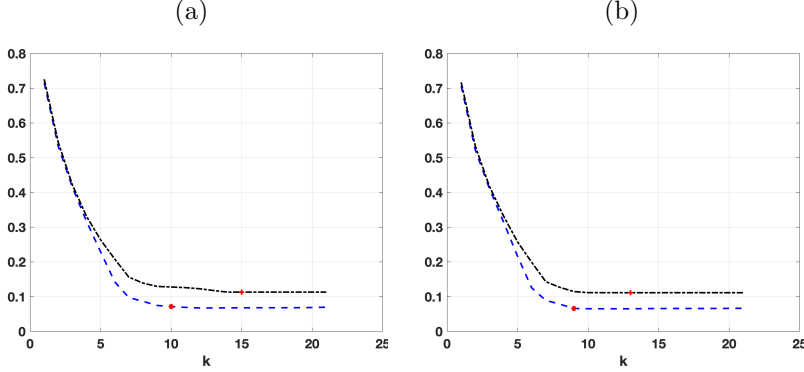


FIG. S3. *Test problem T1* ($\delta = 0.01$). *Relative error curves vs. the iteration index k . (a) Case $\Omega = \mathbb{R}^N$. (b) Case $\Omega = \mathbb{R}_+^N$. The black dash-dot line represents the relative error values of Algorithm UPenMM and the blue dashed line represents the relative error values of Algorithm GUPenMM. The red dots indicate the relative error values corresponding to stopping criterion (2.1).*

tion of the regularization parameters introduced in Algorithm GUPenMM producing smaller relative errors and faster convergence. The plot of the values of the surrogate function is shown in Figure S4, demonstrating that the convergence criterion is met. The good agreement of the residual curves with the noise norm is observed in Figure

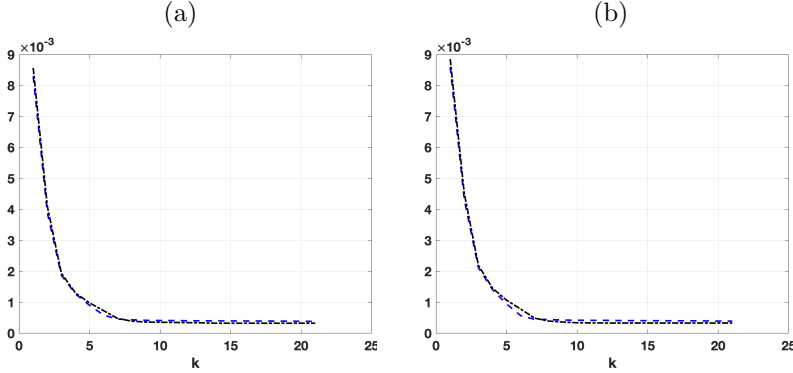


FIG. S4. *Test problem T1* ($\delta = 0.01$). *Value of the surrogate function. (a) $\Omega = \mathbb{R}^N$ (b) $\Omega = \mathbb{R}_+^N$. The black dash-dot line represents the $Q(\hat{\lambda}^{(k+1)}, \lambda^{(k)})$ values in Algorithm UPenMM and the blue dashed line represents the $Q(\tilde{\lambda}^{(k+1)}, \lambda^{(k)})$ values in Algorithm GUPenMM.*

S5 where the black dash-dot line represents the residual norm values in Algorithm UPenMM and the blue dashed line indicates the residual norm values in Algorithm GUPenMM. The red line represents the noise norm. In addition to the error curves, the values in Table S1 and the plots of the reconstructed signals in Figure S6 confirm the superior quality obtained by Algorithm GUPenMM. This feature is even more evident in the case of more complex signals such as those represented by test problems T2 and T3; in these cases, we only represent the reconstructed signals for $\Omega = \mathbb{R}_+^N$ in Figure S7. The computation times presented in Table S2 show the performance of the different methods. The computation times for UPenMM and GUPenMM indicate a relatively stable increase across the test scenarios from T1 to T3. This increment

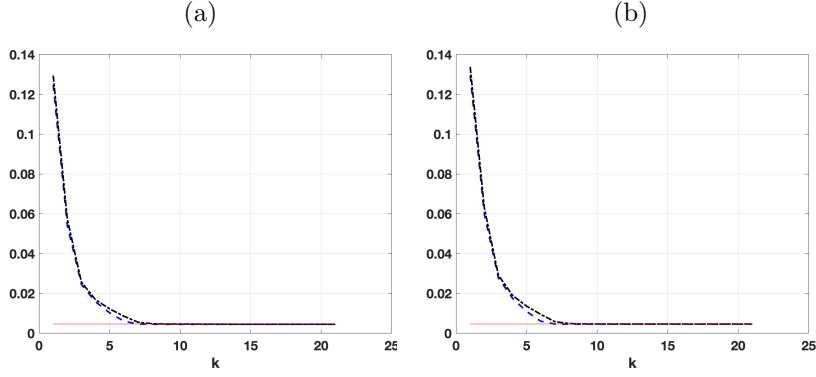


FIG. S5. Test problem T1 ($\delta = 0.01$). Behaviour of the residual norm. (a) $\Omega = \mathbb{R}^N$ (b) $\Omega = \mathbb{R}_+^N$. The black dash-dot line represents the residual norms in Algorithm UPenMM and the blue dashed line is the residual norms in Algorithm GUPenMM. The red line represents the noise norm.

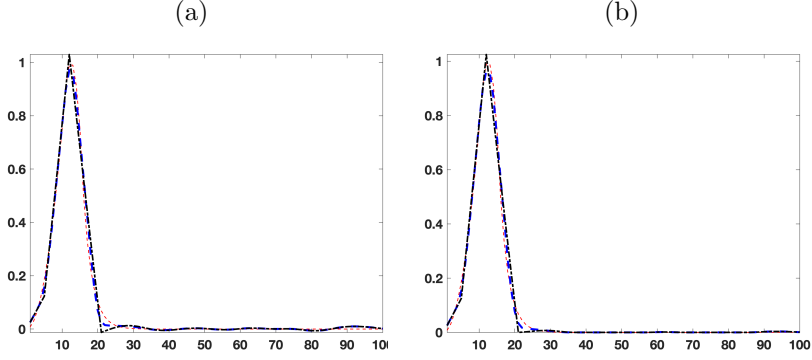


FIG. S6. Test problem T1 ($\delta = 0.01$). Solutions \mathbf{u} . (a) $\Omega = \mathbb{R}^N$ (b) $\Omega = \mathbb{R}_+^N$. The black dash-dot line represents \mathbf{u} computed by Algorithm UPenMM and the blue dashed line represents \mathbf{u} computed by Algorithm GUPenMM. The red dashed line represents the ground-truth solution.

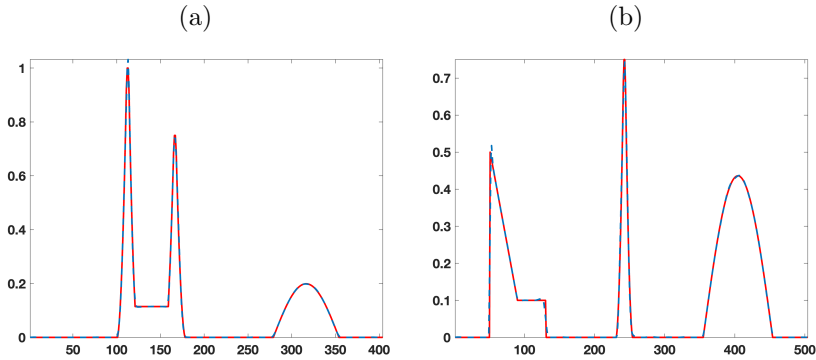


FIG. S7. Solutions \mathbf{u} by Algorithm GUPenMM + (blue dashed line) and ground-truth solution (red dashed line). (a) Test problem T2 ($\delta = 0.01$) (b) Test problem T3 ($\delta = 0.01$).

Method	T1		T2		T3	
	Rel Err	Iters	Rel Err	Iters	Rel Err	Iters
UPenMM	$1.1313 \cdot 10^{-1}$	15	$9.8773 \cdot 10^{-2}$	7	$1.0532 \cdot 10^{-1}$	9
UPenMM +	$1.1136 \cdot 10^{-1}$	13(6)	$8.6412 \cdot 10^{-2}$	6 (42)	$1.0188 \cdot 10^{-1}$	11(47)
GUPenMM	$7.1381 \cdot 10^{-2}$	10	$2.5204 \cdot 10^{-2}$	7	$6.2736 \cdot 10^{-2}$	18
GUPenMM +	$6.5993 \cdot 10^{-2}$	9(48)	$2.7592 \cdot 10^{-2}$	9(66)	$6.1298 \cdot 10^{-2}$	19(65)
L2	$1.1527 \cdot 10^{-1}$	/	$7.9064 \cdot 10^{-2}$	/	$1.0380 \cdot 10^{-1}$	/
L2 +	$7.9265 \cdot 10^{-2}$	/	$6.1054 \cdot 10^{-2}$	/	$8.9234 \cdot 10^{-2}$	/

TABLE S1

1D test problems ($\delta = 0.01$). Relative error and the corresponding number of iterations with $Tol_\lambda = 10^{-2}$. The symbol + indicates the constrained case. Between parenthesis, the number of Newton Projection iterations is reported.

is expected as the size of the test problems increases from T1 to T3. When the non-negativity constraint is present (“+” versions), computation times for T2 and T3 increase in both UPenMM+ and GUPenMM+. Despite this increase, Table S1 shows that the accuracy generally improves. This suggests that the non-negativity constraint, while increasing computation time, enhance the solution’s precision. A

Method	Computation times		
	T1	T2	T3
UPenMM	$3.01 \cdot 10^{-2}$	$5.53 \cdot 10^{-2}$	$1.09 \cdot 10^{-1}$
UPenMM +	$2.70 \cdot 10^{-2}$	$3.00 \cdot 10^0$	$2.75 \cdot 10^0$
GUPenMM	$2.75 \cdot 10^{-2}$	$1.66 \cdot 10^{-1}$	$3.06 \cdot 10^{-1}$
GUPenMM +	$2.78 \cdot 10^{-2}$	$3.00 \cdot 10^0$	$4.86 \cdot 10^0$

TABLE S2

1D test problems ($\delta = 0.01$). Computation times in seconds. The symbol + indicates the constrained case.

final consideration concerns the values of the point-wise regularization parameters. Figure S8 illustrates the characteristic of this method: since all the penalty terms are constant, then the values of the regularization parameters are larger in correspondence with flat areas and become smaller where the solution exhibits rapid changes. The

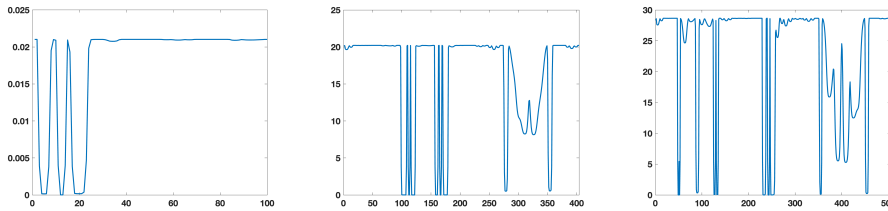


FIG. S8. 1D test problems ($\delta = 0.01$). Regularization parameters computed by GUPenMM. Left T1, center T2, right T3.

last two rows of Table S1 compare the relative errors when utilizing the Tikhonov method with optimal regularization parameter. Figure S9 illustrates that a single parameter, even if optimally weighted, is unable to reconstruct equally well all the details of complex signals presenting many different features (e.g. T2, T3).

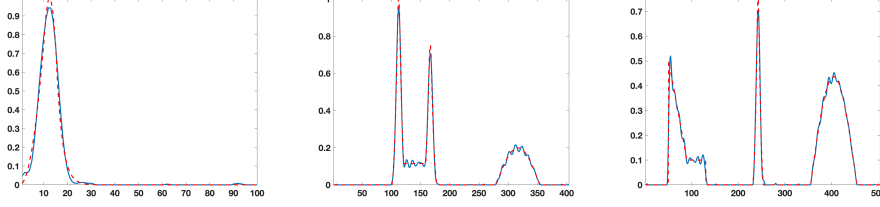


FIG. S9. 1D test problems ($\delta = 0.01$). Method L2+ with optimal regularization parameter. Left T1, $\lambda = 2.7838 \times 10^{-5}$. Center T2, $\lambda = 3.495495 \times 10^{-3}$. Right T3, $\lambda = 3.242424 \times 10^{-3}$.

3. High-noise results. In this section, we present the results obtained with high-noise ($\delta = 0.1$), restricted to the case $\Omega = \mathbb{R}_+^N$, because the absence of the non-negativity constraint produces worse results. Figure S10 shows the blurred noisy data \mathbf{b} (blue line), and the blurred data \mathbf{y} .

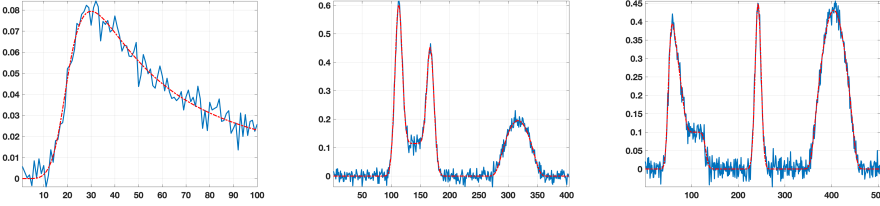


FIG. S10. 1D test problems ($\delta = 0.1$). Blue line: blurred noisy data \mathbf{b} , dashed red line: blurred data \mathbf{y} . Left T1, center T2, right T3.

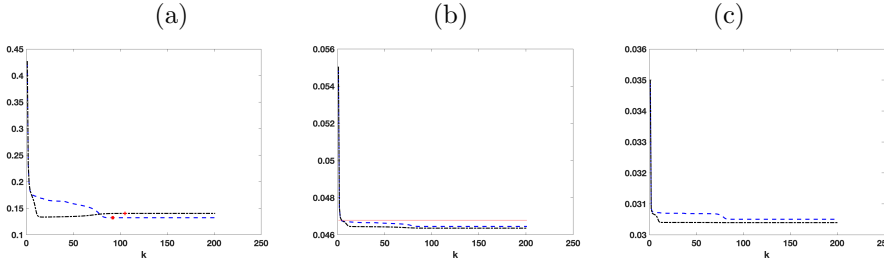


FIG. S11. T1 test problem ($\delta = 0.1$). (a) Relative error curves: Algorithm UPenMM (black dash-dot line) and Algorithm GUPenMM (blue dashed line). Red dots indicate values at the exit criterion (2.1). (b) Residual norm behaviour: Algorithm UPenMM (black dash-dot line), Algorithm GUPenMM (blue dashed line), and noise norm (red line). (c) Surrogate function values: $Q(\tilde{\lambda}^{(k+1)}, \lambda^{(k)})$ for Algorithm UPenMM (black dash-dot line) and $Q(\tilde{\lambda}^{(k+1)}, \lambda^{(k)})$ for Algorithm GUPenMM (blue dashed line).

In Figure S11(a), we represent the relative error curves of Algorithm UPenMM (black dash-dot line) and Algorithm GUPenMM (blue dashed line) for T1. The red dots represent the relative error values corresponding to the **stopping criterion** (2.1) with $Tol_\lambda = 10^{-5}$. Compared to the low-noise case, a smaller value of the tolerance is necessary to stop the algorithms close to their limit. While the error of Algorithm UPenMM decreases more rapidly in the initial iterations, Algorithm GUPenMM achieves a slightly smaller error in the limit. The good agreement of the

residual curves with the noise norm is observed in Figure S11(b) where the black dash-dot line represents the residual norm values in Algorithm UPenMM, the blue dashed line indicates the residual norm values in Algorithm GUPenMM and the red line represents the noise norm. The plot of the values of the surrogate function is shown in Figure S11(c). Figure S12(a) shows the good reproduction of the high

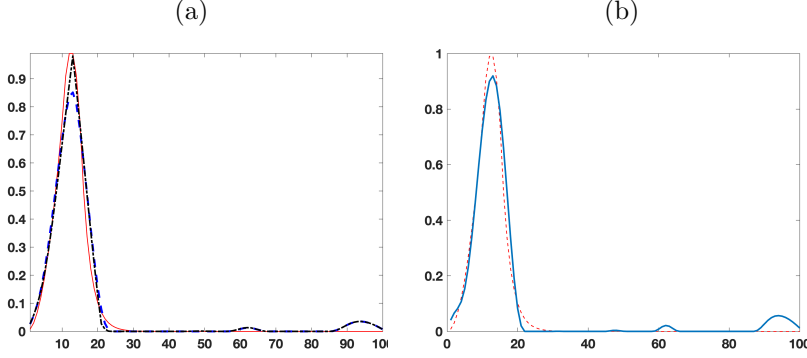


FIG. S12. Test problem T1 ($\delta = 0.1$). Solution \mathbf{u} with $\Omega = \mathbb{R}_+^N$. (a) \mathbf{u} computed by Algorithm UPenMM (black dash-dot line), \mathbf{u} computed by Algorithm GUPenMM (blue dashed line) and ground-truth solution (red dashed line). (b) Solution computed by Tikhonov L2+ (blue line) with optimal parameter $\lambda = 1.5167 \cdot 10^{-3}$, and ground-truth solution (red dashed line).

peak obtained from both algorithms, with spurious oscillations in the flat region that, however, they are less pronounced compared to the Tikhonov L2+ solution with optimal regularization parameter (Figure S12(b)). A similar behaviour is observed in

Method	T1		T2		T3	
	Rel Err	Iters	Rel Err	Iters	Rel Err	Iters
UPenMM +	$1.401 \cdot 10^{-1}$	105(169)	$1.081 \cdot 10^{-1}$	14(72)	$1.093 \cdot 10^{-1}$	15(89)
GUPenMM +	$1.323 \cdot 10^{-1}$	92(171)	$8.068 \cdot 10^{-2}$	84(241)	$1.072 \cdot 10^{-1}$	361(825)
L2 +	$1.427 \cdot 10^{-1}$	/	$1.019 \cdot 10^{-1}$	/	$1.270 \cdot 10^{-1}$	/

TABLE S3

1D test problems ($\delta = 0.1$). Relative error and the corresponding number of iterations with $Tol_\lambda = 10^{-5}$. The symbol + indicates the constrained case. Between parenthesis, the number of Newton Projection iterations is reported.

tests T2 and T3, as depicted in Figures S13 and S14. Table S3 shows that the smallest relative error is obtained by Algorithm GUPenMM (row GUPenMM +) in each case and that Tikhonov L2+ produces the worst results. Figure S15 represents the point-wise regularization parameter, confirming the characteristics already observed in the low-noise case. Finally, concerning the computation times reported in Table S4, we observe higher values compared to the low-noise case (Table S2) due to the use of a smaller tolerance ($Tol_\lambda = 10^{-5}$ vs $Tol_\lambda = 10^{-2}$ with low noise). Additionally, GUPenMM + is more expensive compared to UPenMM +.

REFERENCES

- [1] P. C. HANSEN, *Regularization tools version 4.0 for Matlab 7.3*, Numerical algorithms, 46 (2007), pp. 189–194.

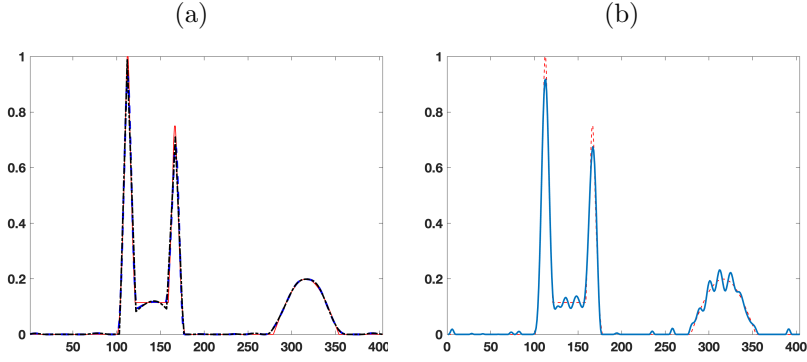


FIG. S13. Test problem T2 ($\delta = 0.1$). Solution \mathbf{u} with $\Omega = \mathbb{R}_+^N$. (a) \mathbf{u} computed by Algorithm UPenMM (black dash-dot line), \mathbf{u} computed by Algorithm GUPenMM (blue dashed line) and ground-truth solution (red dashed line). (b) Solution computed by Tikhonov L2+ (blue line) with optimal parameter $\lambda = 7.2326 \cdot 10^{-2}$, and ground-truth solution (red dashed line).

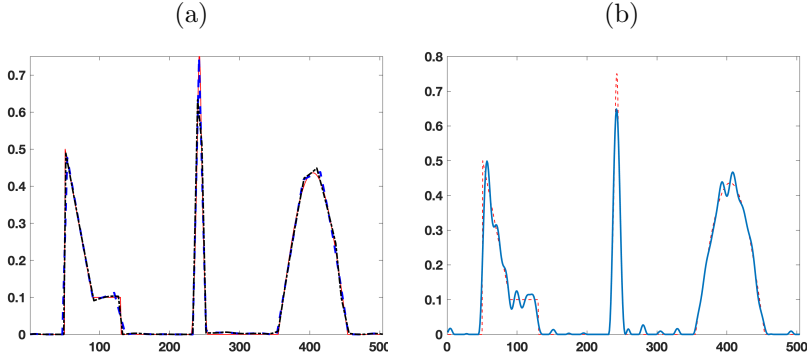


FIG. S14. Test problem T3 ($\delta = 0.1$). Solution \mathbf{u} with $\Omega = \mathbb{R}_+^N$. (a) \mathbf{u} computed by Algorithm UPenMM (black dash-dot line), \mathbf{u} computed by Algorithm GUPenMM (blue dashed line) and ground-truth solution (red dashed line). (b) Solution computed by Tikhonov L2+ (blue line) with optimal parameter $\lambda = 6.0103 \cdot 10^{-1}$, and ground-truth solution (red dashed line).

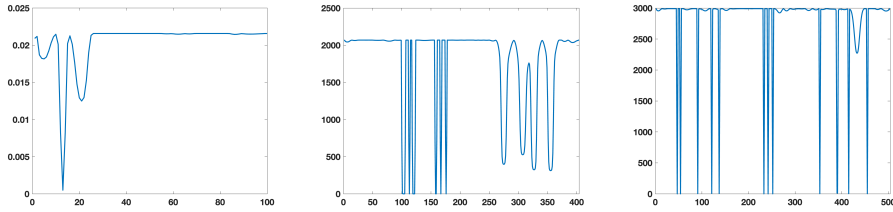


FIG. S15. 1D test problems ($\delta = 0.1$). Regularization parameters computed by GUPenMM. Left T1, center T2, right T3.

[2] D. BERTSEKAS, *Nonlinear Programming*, Athena Scientific, (2nd Edition), 1999.

Method	Computation times		
	T1	T2	T3
UPenMM +	$5.61 \cdot 10^{-2}$	$3.02 \cdot 10^0$	$5.58 \cdot 10^0$
GUPenMM +	$7.57 \cdot 10^{-2}$	$9.36 \cdot 10^0$	$4.50 \cdot 10^1$

TABLE S4

1D test problems ($\delta = 0.1$). Computation times in seconds. The symbol + indicates the constrained case.